

Non-Consensus Opinion Model with Byzantine Nodes

Xinhan Liu*, Massimo A. Achterberg*, Robert E. Kooij*[†]

*Faculty of Electrical Engineering, Mathematics and Computer Science, Delft University of Technology, Delft, The Netherlands

[†]TNO, Unit ICT, The Netherlands

email: liuxinhan96@gmail.com, {M.A.Achterberg, R.E.Kooij}@tudelft.nl

Abstract—Opinion dynamics models study how the interaction among people influences the opinion formation process. In most opinion dynamics models, only one opinion can exist in the steady state, which is different from the real-life opinion formation process. In 2009, Shao *et al.* introduced a Non-Consensus Opinion (NCO) model, which allows different opinions to coexist in the steady state. This paper extends the NCO model by introducing a special type of nodes, namely Byzantine nodes, to play the role of dishonest people. We perform simulations on three different network models: small-scale graphs, Erdős–Rényi random graphs and scale-free networks. We find a new steady state for the NCO model: the cyclic steady state. The cyclic behavior of the NCO and Byzantine NCO model is discussed, including a method to generate networks with extremely long cycle lengths. Other properties of the Byzantine NCO model, such as the probability of cyclic behavior and the final opinion distribution, are also studied. We find that the introduction of Byzantine nodes generally steers towards a more balanced steady state and increases the probability of cyclic behavior. The latter is particularly problematic in communication systems, where the large cycle lengths may cause a very slow consensus process and thus stalling future communications.

Index Terms—Opinion models, Complex Networks, Social Dynamics model, Byzantine nodes.

I. INTRODUCTION

In recent years, the study of social dynamics and group behavior has been greatly developed. Of great concern is the spread of opinions in social networks [1]–[3]. Opinion dynamics is driven by human behavior and includes many elements, such as individual predisposition, the influence of other people (social networks playing a crucial role in this respect), and many others. Different models have been developed, encompassing different elements of the opinion formation process.

Most of the opinion models are based on spin models, such as the Sznajd model [4], the voter model [5], the majority rule model [6] and the social impact model [7]. These opinion models use insights from complex network theory, where nodes in the network represent people and links denote a relationship between people. A drawback of conventional spin models is that they usually result in a consensus steady state, while in real life, different opinions tend to coexist in the steady state [1], [8].

In 2009, Shao *et al.* proposed the Non-Consensus Opinion model (NCO) model, which can be used to research the

opinion dynamics of a group of people [9]. The NCO model describes the spread of two opinions σ_+ and σ_- in a network, where each node always has one of the two possible opinions. Each node re-considers its own opinion at every discrete time step by looking at the opinions of all its neighbors and its own opinion. If the majority opinion is different from its current opinion, the node reverts to the other opinion. If there is no majority opinion or if the majority is equal to the node's opinion, the node's opinion does not change.

Unlike models based on spin systems, the NCO model allows for non-consensus steady states. Shao *et al.* illustrates the important fact that the NCO model is similar to the invasion percolation process [10], which means that if the number of people holding the minority opinion is sufficiently large, the minority opinion holders can form a stable cluster, which the dominant opinion cannot invade.

Despite the fact that Shao *et al.*'s classic NCO model solves the problem of coexisting opinions in the steady state, the NCO model still cannot ideally mimic the opinion formation process because people do not always behave like the nodes in the NCO model. In 2011, Li *et al.* proposed an inflexible contrarian opinion (ICO) model by introducing stubborn agents who never change their opinion [11]. Li *et al.*'s study makes the NCO model more relevant to real-life social networks. Li *et al.* proposed the NCOW model [8] by added a weighting factor W to the NCO model. The weighting factor W for each node represents the importance of that person's opinion in the decision-making process. Hence, a large W makes that node's opinion hard to change.

The NCO model assumes that all nodes are honest and reliable, but we always meet rascals who lie and make trouble in real life. In this paper, we extend the NCO model to the Byzantine NCO model. In the Byzantine NCO model, the Byzantine node is introduced, which is a new type of node that plays the role of a liar in a crowd [12]. Unlike ordinary nodes, Byzantine nodes always communicate the opposite of their true opinion. Byzantine nodes are often used for modelling hacked nodes in security systems and communication networks [13]. One method to detect Byzantine nodes is using opinion models [14], [15]. Having a thorough understanding of the Byzantine NCO model can help to improve the Byzantine node detection algorithm. In particular, we will show that adding

Byzantine nodes will delay the opinion formation process, increase the probability of cyclic behavior and the final opinion fraction is more balanced than without Byzantine nodes.

We start by introducing the NCO model with Byzantine nodes in Section II. We show examples of cyclic behavior in Section III and present a method to construct very long cycle lengths. We discuss the opinion fraction at the steady state in Section IV and explain how different strategies for selecting Byzantine nodes influence the opinion fraction at the steady state in Section V. Finally, we conclude in Section VI.

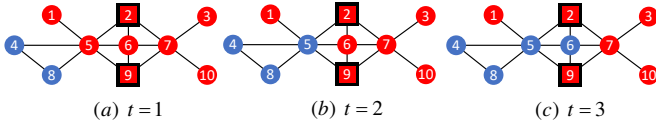


Fig. 1. Dynamics of the Byzantine NCO model on a network with $N = 10$ nodes. Node 2 and 9 are Byzantine nodes, as indicated by the thick, black border around the square node. The other nodes are normal nodes, indicated by circles. (a) At $t = 1$, 8 nodes are assigned with a σ_+ opinion (red), and other nodes with a σ_- opinion (blue). Byzantine node 2 and node 9 hold a σ_+ opinion, but they declare a σ_- opinion. This make node 5 to misjudge its local opinion ratio as $\sigma_+ : \sigma_- = 3 : 4$. Node 5 converts to σ_- . (b) At $t = 2$, node 6 judges its local opinion ratio as $\sigma_+ : \sigma_- = 2 : 3$ and node 6 converts to σ_- . (c) At $t = 3$, all nodes hold an opinion that they consider to be a local majority and stop changing their opinions. The system has reached a steady state.

II. THE BYZANTINE NCO MODEL

In the NCO model, nodes choose their opinions according to their own current opinion and that of their neighbors. At each discrete time t , each node looks at the opinion of its nearest neighbors in the graph and its own opinion. If the majority opinion is different from its current opinion, the node reverts to the other opinion. The NCO model is an example of a discrete-time model with synchronous updates, because each node simultaneously decides to keep or to change its opinion. The Byzantine NCO model introduces Byzantine nodes to the NCO model, where the Byzantine nodes always declare an opinion opposite to their true opinion. Fig. 1 shows an example of the dynamics in the Byzantine NCO model. Note that regular, i.e. non-Byzantine nodes are depicted as filled circles, while Byzantine nodes are shown as filled squares, with a thick black border.

Throughout this work, we simulate the NCO model on three different kinds of network models: All graphs with $N = 7$ nodes and $L = 10$ links (there are 132 non-isomorphic graphs generated from Nauty and Traces [16]), Erdős–Rényi random graphs with $N = 100$ and $p = 0.047$ and Barabási-Albert scale-free networks with $N = 100$, $\lambda = 3$ and $k_{\min} = 2$. On the graphs with $N = 7$ nodes and $L = 10$ links, we perform an exhaustive operation, where all the $2^7 = 128$ different initial configurations and all the $2^7 = 128$ different Byzantine node positions are taken into consideration. Initially on the ER and SF networks, opinion σ_- and σ_+ are randomly assigned to all the N nodes with a fraction of f and $1 - f$, respectively.

Out of all nodes, N_B nodes are chosen as Byzantine nodes according to one of the following strategies:

- 1) Strategy I: Randomly select N_B nodes to be Byzantine nodes.
- 2) Strategy II: Select N_B nodes with highest degree to be Byzantine nodes.
- 3) Strategy III: Select N_B nodes with lowest degree to be Byzantine nodes.

We perform simulations until the system reaches a fixed steady state or ends up in a cyclic steady state.

III. CYCLIC BEHAVIOR

In a previous study of the NCO model [9], researchers believe that the opinion network eventually reaches a fixed steady state. In the fixed steady state, the opinion of each node in the network becomes fixed, and the opinion network shows a state of consensus (all nodes are of the same opinion) or coexistence (both opinions coexist). However, in a few cases, the opinion of some nodes in the opinion network do not reach a fixed steady state. Instead, the whole network constantly oscillates between two different states. We refer to this phenomenon as *cyclic behavior*.

The cyclic behavior of the NCO model is relatively simple, because only cycles with length two have been found. We show an example of cyclic behavior in the NCO model in Fig. 2. Nodes 1, 2 and 3 form one group, node 5 and 6 form another group and each node in each group keeps changing its opinion after each time step. In this example, the opinion of node 4 is unchanged.

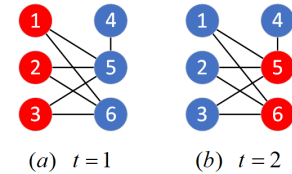


Fig. 2. Dynamics of a cycle of the NCO model. (a) At $t = 1$, node 1, 2 and 3 have two σ_- neighbors node 5 and 6, so their local opinion ratio is $\sigma_+ : \sigma_- = 1 : 2$. Node 5 has 3 σ_+ neighbors and 1 σ_- neighbor; node 6 has 3 σ_+ neighbors. The local opinion ratio for node 5 and 6 are $\sigma_+ : \sigma_- = 3 : 2$ and $\sigma_+ : \sigma_- = 3 : 1$, so node 5 and 6 change their opinion. (b) At $t = 2$, node 1, 2 and 3 have two σ_+ neighbors node 5 and 6, so their local opinion ratio is $\sigma_+ : \sigma_- = 2 : 1$. Node 5 has 5 σ_- neighbors; node 6 has 3 σ_- neighbor. The local opinion ratio for node 5 and 6 are $\sigma_+ : \sigma_- = 1 : 4$ and $\sigma_+ : \sigma_- = 1 : 3$, so node 5 and 6 change their opinion. Then the system switches back to the state at $t = 1$.

Unlike regular nodes, Byzantine nodes always declare the opposite of their own opinion. Normal nodes drive the network to a consensus state, while Byzantine nodes drive the network to a balanced opinion state. For example, when the network seems to converge to the positive opinion consensus state, the sudden change of the opinion of a Byzantine node may steer the network towards the negative opinion. The Byzantine nodes make it easier for the network to oscillate between two opinions. This property of Byzantine nodes makes the Byzantine NCO model more prone to cyclic behavior with

long cycle lengths. Fig. 3 shows an example of a network with a cycle length of 6.

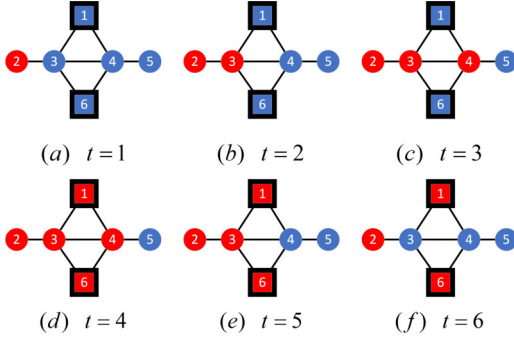


Fig. 3. Cyclic behavior in the Byzantine NCO model. The cycle length is 6 because the network state at $t = 7$ is equal to the network state at $t = 1$.

To our best knowledge, cycles with a length larger than two do not exist in the NCO model. But the introduction of Byzantine nodes allows for longer cycles, as e.g. shown in Fig. 3. There is, in general, no mathematical formula for the cycle length for a given network with a certain initial opinion configuration. However, we found some fascinating cases while studying cyclic steady states, and selected a few to show.

A. Sunflower Graphs

In this section we consider so-called sunflower graphs, defined on $2M$ nodes. To construct a sunflower graph, we start with a ring graph, consisting of M Byzantine nodes. Then M regular nodes are added, such that each regular node connects to two adjacent Byzantine nodes, see Fig. 4. As initial condition, one Byzantine node and an adjacent regular node are assigned the positive opinion σ_+ and all other nodes start with the negative opinion σ_- .

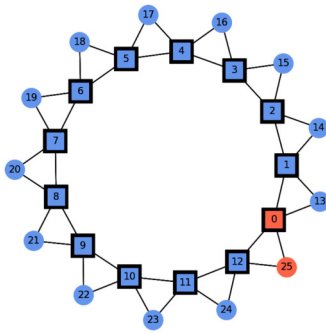


Fig. 4. A sunflower graph with $N = 26$ nodes, $L = 39$ links and $N_B = 13$ Byzantine nodes. The cycle length of this graph is 52.

The cycle length for sunflower graphs with N nodes, where N is an even integer not less than 6, satisfies

$$C_{\text{sunflower graph}} = \begin{cases} N & \text{if } N/2 \text{ is an even number} \\ 2N & \text{if } N/2 \text{ is an odd number} \end{cases} \quad (1)$$

Using sunflower graphs, we can generate networks with a cycle length of $4n$ ($n \geq 2, n \in \mathbb{N}$).

B. Chain of diamond graphs

The cycle length of the sunflower graph increases linearly with the number of nodes. We also found a network with a nonlinear increase in the cycle length as a function of the number of Byzantine nodes. This network consists of a chain of connected diamond-like graphs. Each diamond graph, denoted by D , consists of a path of 5 regular nodes, where each of the regular nodes is connected to a pair of Byzantine nodes. Depending on how the diamond graphs are connected, we can divide the special graphs into two types.

1) *Type I*: The outer nodes of a diamond graph are chained with another diamond graph, as shown in Fig. 5. At the initial state, the leftmost regular node holds a σ_+ opinion, while all other nodes hold a σ_- opinion.

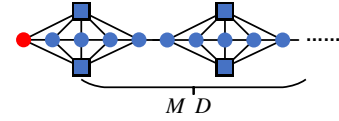


Fig. 5. Graph type I with M normal diamond graphs D chained together.

2) *Type II*: To generate a Type II graph, we first connect M diamond graphs using the method in Type I, then E diamond graphs are added where one outer regular node in the new diamond graph is connected with one Byzantine node in the last diamond graph in the existing network, as depicted in Fig. 6.

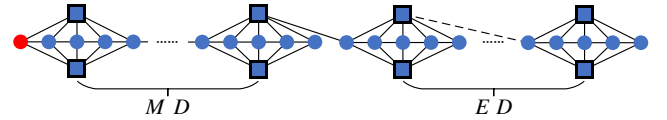


Fig. 6. Graph type II with M normal diamond graphs D and E differently connected diamond graphs D .

Table I gives the cycle length for chains of diamond graphs, of several lengths. When $M = 21$ and $E = 1$ (resulting in a graph on $22 \times 7 = 154$ nodes), the cycle length reaches 22131760. Using diamond graphs, we use fewer nodes to achieve long cycles compared to sunflower graphs. Even for the regular diamond graphs without any type II connections, the cycle length pattern in Table I is highly irregular and it is presumably very hard to derive a general formula.

C. Network combination

We propose *network combination* as another method to generate networks with long cycle lengths. The idea is that we combine several different networks into one connected network, without breaking the cyclic behavior of each component. However, connecting the components directly can easily break the cyclic behavior of each individual graph. Thus, we also add

TABLE I
CYCLE LENGTH FOR GRAPHS CONSISTING OF CONCATENATED DIAMOND GRAPHS D . FOR $E = 0$, THE GRAPH ONLY CONSISTS OF TYPE I CONNECTIONS.

Number of D (M+E)	2	3	4	5	6	7	8
Cycle length ($E = 0$)	10	1	20	26	102	136	28
Cycle length ($E = 1$)	1	1	1	38	1,178	520	174
Cycle length ($E = 2$)		1	10	1	190	664	366
Cycle length ($E = 3$)			1	10	1	190	170
Number of D (M+E)	9	10	11	12	13	14	15
Cycle length ($E = 0$)	3,372	28	2,615	4,644	179	1,113	28
Cycle length ($E = 1$)	5,388	864	11,832	612	45,918	110,490	56,022
Cycle length ($E = 2$)	402	4,796	9,514	24,620	38,360	69,602	61,308
Cycle length ($E = 3$)	1	7,152	1,490	6,320	89,974	26,449	93,278
Number of D (M+E)	16	17	18	19	20	21	22
Cycle length ($E = 0$)	18	179	5,682	28	126	28	3,769,654
Cycle length ($E = 1$)	756	179	347,177	179	6,620,424	722,301	22,131,760
Cycle length ($E = 2$)	566,850	390,278	1,952,400	314,951	76,835	5,000,520	8,229,700
Cycle length ($E = 3$)	128,010	89,352	255,249	918,374	1,138,078	1,207,604	11,880,976

a mirror of each component with the opposite initial opinion. We then connect two adjacent components and their mirrors by adding two links, such that each component is connected to its neighbors and their mirrors, but not to its own mirror. Fig. 7 demonstrates how five components are connected together without breaking the cycles of each individual component. The cycle length of the combined network is the least common multiple of the cycle lengths of the components.

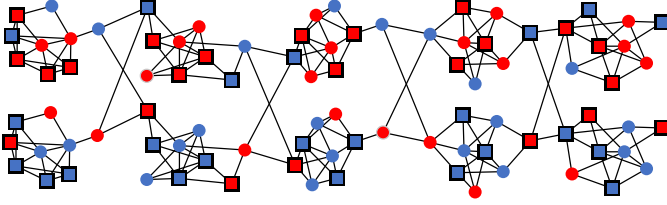


Fig. 7. The combined network is created by connecting five graphs (and their mirrors), whose individual cycle lengths are 17, 19, 21, 23 and 50. The combined network has a cycle length of $lcm(17, 19, 21, 23, 50) = 7800450$.

In this way, one can connect an arbitrary number of components. The sunflower graphs provide us with networks with a cycle length of $4n$, where $n \geq 2$ is a positive integer. The least common multiple of prime numbers is the product of them. Combining m sunflower graphs with cycle lengths $4n_1, 4n_2, \dots, 4n_m$, where n_1, n_2, \dots, n_m are all distinct prime numbers, we obtain a combination network with a cycle length of $lcm(4n_1, 4n_2, \dots, 4n_m) = 4 \times \prod_{i=1}^m n_i$, while using only $2 \times (N_1 + N_2 + \dots + N_m)$ nodes.

The large cycle lengths are of great concern in communication networks, where a consensus must be reached. Byzantine nodes may disrupt the opinion formation process, leading to extremely long communication times which may stall all future communications. The way forward is to design communication networks that can withstand these Byzantine attacks, but this is outside of the scope of this paper.

D. Occurrence of the cyclic behavior

The introduction of Byzantine nodes not only produces long cycles, but also increases the probability of cyclic behavior.

Fig. 8 illustrates the probability of cyclic behavior p_c on ER networks with $N = 100$, $p = 0.047$ as a function of the initial negative opinion fraction f , for a different number of Byzantine nodes. From Fig. 8a, we find that for the NCO model without Byzantine nodes, the $p_c(f)$ curve has a peak at $f = 0.5$ and the networks show cyclic behavior in the interval $(0.39, 0.61)$, which roughly overlaps with the interval of the coexistence steady state (see Section IV). In Fig. 8b, when there are 10 Byzantine nodes, the cyclic behavior occurs in a wider interval. In Fig. 8c, as the number of Byzantine nodes N_B increases, the p_c curve shows a ‘W’-shape; both the middle and the left and right sides show a relatively high p_c . In Fig. 8d, when almost all nodes are Byzantine, the peak is situated at the left and right side. In the side area where f is close to $f = 0$ or $f = 1$, most nodes in the network start with the same opinion. Due to the lying nature of the Byzantine nodes, most nodes in the network will misjudge the local majority opinion and thus change their opinion, at which the minority opinion becomes the majority opinion. The node’s opinion will continue to change, oscillating between the two opinions and reaching a cyclic steady state.

IV. OPINION FRACTION AT STEADY STATE

For the NCO model, the final opinion fraction is an essential element of steady-state behavior because the final opinion fraction reflects which opinion is the majority opinion in the steady state. Shao *et al.* finds that there is a critical threshold f_c that distinguishes between consensus and coexistence in the steady state [9]. For $f < f_c$, the network tends to reach a consensus whereas both opinions tend to coexist if $f > f_c$.

The final opinion fraction F is defined as the fraction of nodes holding a specific opinion among all nodes when the NCO model reaches a steady state, denoted as

$$F = n_{\sigma_-} / N \quad (2)$$

where n_{σ_-} is the number of nodes holding the σ_- opinion and N is the total number of nodes in the network.

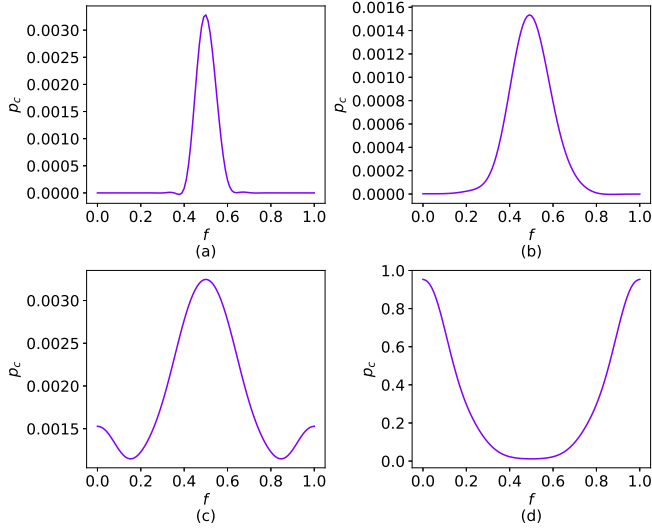


Fig. 8. The probability of occurrence of cyclic behavior p_c as a function of the initial fraction f of σ_- opinion on ER networks with $N = 100$, $p = 0.047$, and the placement of Byzantine nodes follows Strategy I for (a) no Byzantine nodes, (b) 10 Byzantine nodes, (c) 20 Byzantine nodes and (d) 90 Byzantine nodes.

In the cyclic steady state, we define the final opinion fraction as the mean value of the opinion fraction of each state in the cycle:

$$F = \frac{\sum_{t=1}^C n_{\sigma_-,t}/N}{C} \quad (3)$$

where C is the length of the cycle and $n_{\sigma_-,i}$ is the number of nodes holding the σ_- opinion at the i^{th} state in the cycle.

We first perform simulations on the small graphs with $N = 7$ nodes and $L = 10$ links. Fig. 9a shows the distribution of the fraction of nodes with the negative opinion σ_- at the steady state for the network without Byzantine nodes. The orange curve and the red violin plot show the mean value and the probability density of the F at different values of f , respectively. We find that F is a monotonically increasing function of f with a symmetry around $(f, F) = (0.5, 0.5)$. For $f \in \{0, 1/7, 2/7\}$, σ_- is the minority opinion and the network tends to reach a positive consensus, with only a few exceptions. The coexistence probabilities in Fig. 9a show a sharp increase for F at $f = 2/7$ to $f = 3/7$. For $f \in \{3/7, 4/7\}$, the majority and minority opinion are close in number and both opinions coexist in most cases.

Fig. 9b shows that for $f = 0$ the main lobe of the violin plot is around $F = 0$, which means that for graphs with no Byzantine nodes, the graph almost always reaches a consensus when one opinion holds an absolute majority position. However, for $f \in \{1/7, 2/7\}$, the main lobes are located in $F \in [1/7, 6/7]$, which means it is hard to reach consensus when Byzantine nodes are added. As more and more Byzantine nodes are added to the system, Fig. 9c and Fig. 9d show that the main lobes of the violin plot are all located in the coexistence area. When there are many Byzantine nodes, the system reaches a

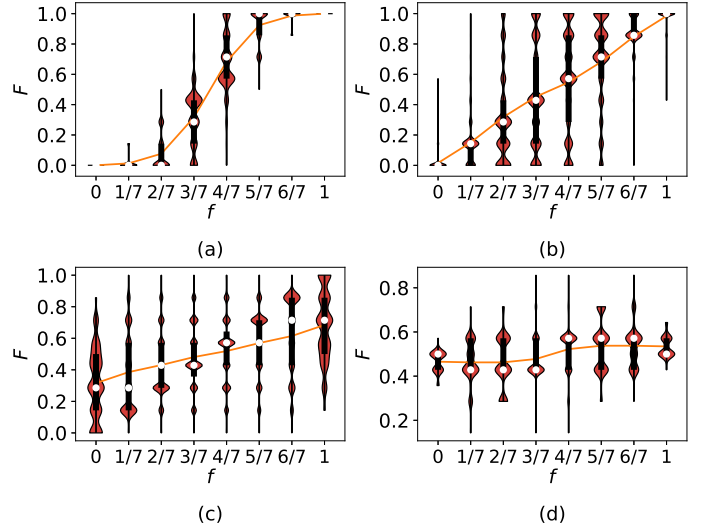


Fig. 9. Violin plot of graphs with $N = 7$, $L = 10$, the orange line shows the average value of F for different f , the red area shows the distribution of F for different f . The white point is the median of F for different f . (a) $N_B = 0$, (b) $N_B = 2$, (c) $N_B = 4$, (d) $N_B = 7$.

coexistence state, regardless of the initial opinion fraction f . When all the nodes are Byzantine nodes, as shown in Fig. 9d, it is impossible for the system to reach a consensus state. Thus, the introduction of Byzantine nodes balances the fraction of different opinions in the steady state. For the Byzantine NCO model, coexistence is a more stable state than consensus when a significant number of nodes are Byzantine nodes.

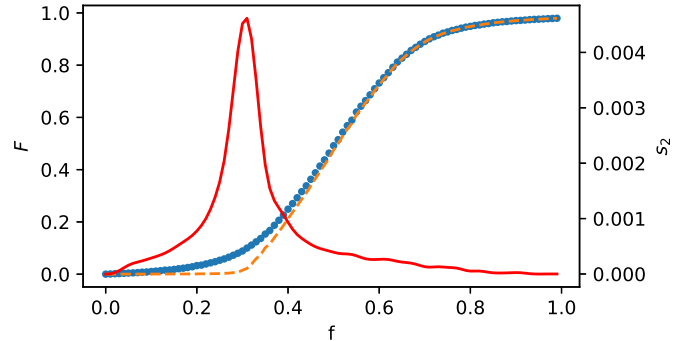


Fig. 10. Normalized size of the largest cluster s_1 (orange dashed line), the second-largest cluster s_2 (red full line) and the fraction of σ_- nodes F (blue dots) in the steady state for an ER network with $N = 10000$ and $p = 0.0004$ without Byzantine nodes.

Fig. 10 shows the normalized size of the largest and second-largest cluster s_1 , s_2 and final opinion fraction F . Shao *et al.* [9] showed that, when the initial fraction of one opinion is below a certain critical threshold f_c , which is characterized by the sharp peak of s_2 , s_1 approaches 0, which means only the majority opinion can form a stably existing cluster. Once f is above f_c , s_1 increases sharply with f . Even though the negative opinion is still the minority, a large, stable minority opinion cluster is formed, which cannot be penetrated by the

positive opinion. Thus, a steady state with stable coexistence of minority and majority opinion appears [9].

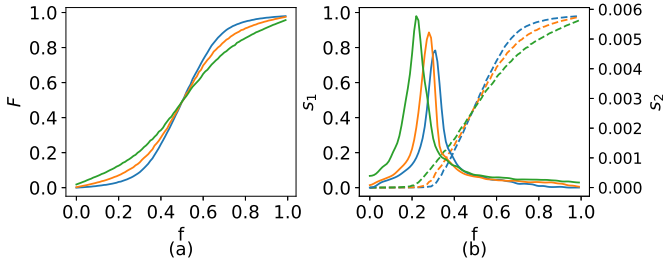


Fig. 11. (a) The final fraction of σ_- nodes F and (b) the normalized size of the largest cluster s_1 (dashed line) and second-largest cluster s_2 (full line) for ER networks with $N = 10000$, $p = 0.0004$ and no Byzantine nodes (blue line), 1000 Byzantine nodes (orange line) and 2000 Byzantine nodes (green line).

Fig. 11 gives the final opinion fraction F and the normalized size of the largest and second-largest σ_- cluster s_1 and s_2 on ER networks with $N = 10000$ and $p = 0.0004$. Increasing the number of Byzantine nodes in Fig. 11 flattens the F curve and moves the peak of the s_2 curve to the left. This indicates that the introduction of Byzantine nodes balances the opinion fractions at the steady state and reduces the value of the critical threshold f_c , which is the smallest f needed to form a stably existing minority opinion cluster.

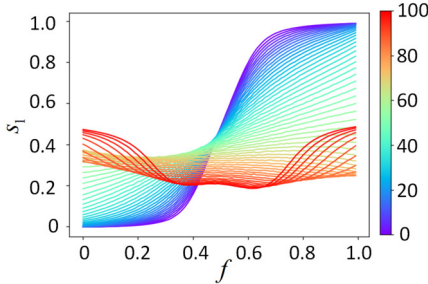


Fig. 12. Normalized size of the largest cluster s_1 for ER networks with $N = 100$, $p = 0.047$ and the number of Byzantine nodes varies between 0 and 100.

Fig. 12 and Fig. 13 depict the normalized size of the largest and second-largest cluster s_1 and s_2 for ER networks with $N = 100$, $p = 0.047$ and the number of Byzantine nodes is varied between 0 and 100. As the number of Byzantine nodes increases, the critical threshold f_c in Fig. 13 moves to the left. When there are only a limited number of Byzantine nodes in the system, consensus remains possible but becomes rarer as the number of Byzantine nodes increases. For a larger number of Byzantine nodes $N_B \geq 40$, the s_2 curve no longer shows an obvious peak in $f \in [0, 1]$ and $s_1(f)$ does not approach 0 in $f \in [0, 1]$. Hence, the network tends to reach a coexistence steady state for any initial opinion fraction f and a minority opinion cluster can stably exist for all $f \in [0, 1]$. If N_B is further increased, i.e. for $N_B \geq 70$, Fig. 13 shows that $s_2(f)$ again has a clear peak but this time it does not correspond with transition for $s_1(f)$, as is clear from Fig. 12.

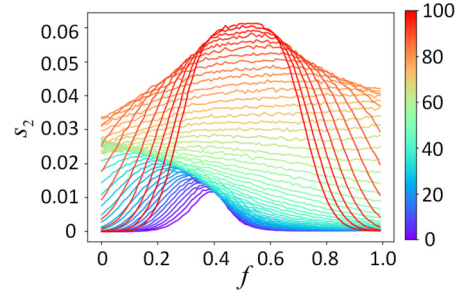


Fig. 13. Normalized size of the second-largest cluster s_2 for ER networks with $N = 100$, $p = 0.047$ and the number of Byzantine nodes varies between 0 and 100.

Fig. 12 shows that the maximum value of s_1 becomes smaller and smaller, while increasing the number of Byzantine nodes. This indicates that the maximum size of the largest clusters in the network becomes smaller. Thus, the introduction of Byzantine nodes prevents the formation of large majority opinion clusters. When there is a significant number of Byzantine nodes, the normalized largest cluster s_1 is no longer a monotonically increasing curve because of the increased probability of cyclic behavior around $f = 0$ and $f = 1$.

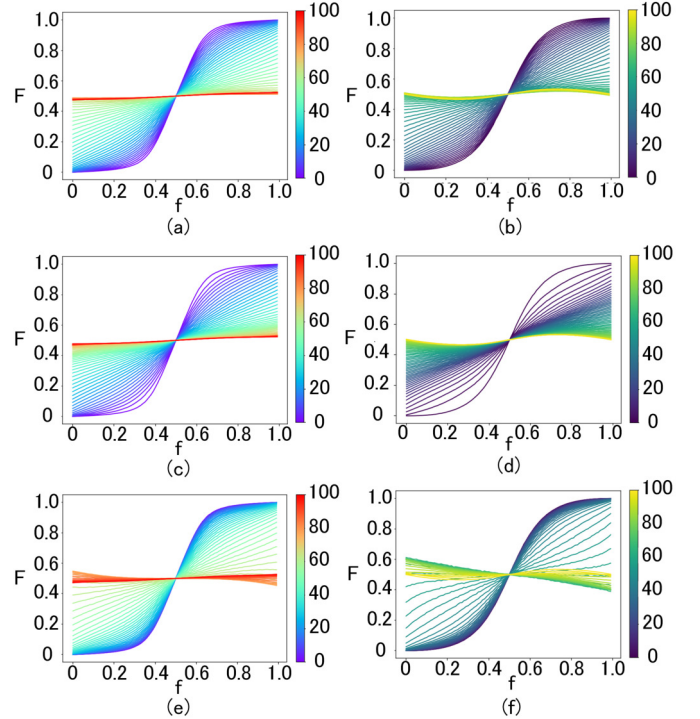


Fig. 14. The final opinion fraction F for (a,c,e) ER networks with $N = 100$, $p = 0.047$ and (b,d,f) SF networks with $N = 100$, $k_{\min} = 2$, $\lambda = 3$. The number of Byzantine nodes N_B is varied between 0 and 100 and is selected according to (a,b) Strategy I, (c,d) Strategy II and (e,f) Strategy III.

V. BYZANTINE NODE SELECTION STRATEGIES

So far, we have selected the Byzantine nodes randomly in the network (according to Strategy I, see Sec. II). Additionally,

we select nodes to be Byzantine based on the largest degree (Strategy II) and lowest degree (Strategy III). Fig. 14 depicts the final opinion fraction F for ER and SF networks for the different Byzantine nodes selection strategies. Comparing the top row (random selection) to the bottom row (lowest degree) of Fig. 14, the curves in the bottom plots with a small number of Byzantine nodes are close together, implying that Byzantine nodes with a low degree have little influence on the final opinion fraction. On the other hand, the middle row suggests that high-degree nodes have a much larger impact on the final opinion fraction F . We conclude that a Byzantine node with more neighbors has more chance to propagate the opposite opinion than a Byzantine node with fewer connections.

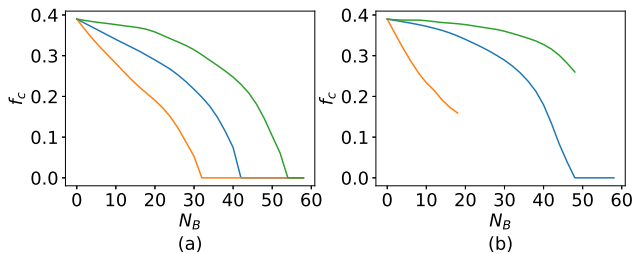


Fig. 15. The critical threshold f_c as a function of Byzantine node number N_B on (a) ER networks with $N = 100$, $p = 0,047$ and (b) SF networks with $N = 100$, $k_{\min} = 2$, $\lambda = 3$ for Strategy I (blue curve), Strategy II (orange curve) and Strategy III (green curve).

Fig. 15 shows how the critical threshold f_c on ER networks ($N = 100$, $p = 0.047$) and SF networks ($N = 100$, $k_{\min} = 2$, $\lambda = 3$) changes with the number of Byzantine nodes N_B . Both for the ER and SF network, the critical thresholds f_c change fastest when strategy II is taken and slowest for strategy III. For ER networks, the critical threshold f_c disappears (i.e. reaches zero) if the number of Byzantine nodes equals 42, 34 and 54 for strategy I, II and III, respectively. For SF networks, the critical threshold f_c reaches 0 only when strategy I is taken. For strategy II, the critical threshold first decreases rapidly, and then becomes unmeasurable due to the increase in probability of cyclic behavior. For strategy III, the critical threshold f_c decreases slowly and then also becomes unmeasurable due to the large probability of cyclic behavior. Taking $N_B \in [0, 20]$, we find that using different Byzantine node selection strategies is more significant for SF networks than for ER networks. The reason is that the degree distribution of ER networks is binomially distributed, while SF networks possess some high-degree nodes. Byzantine nodes with a large degree have a more significant influence on the behavior of the Byzantine NCO model. Due to the larger degree variation in SF networks, following strategy II and strategy III have a larger impact for SF networks than for ER networks.

VI. CONCLUSION

In this paper, we extended the Non-Consensus Opinion (NCO) model proposed by Shao *et al.* [9]. We introduced Byzantine nodes into the NCO model and studied the cyclic behavior of the Byzantine NCO model and the opinion fraction

at the steady state. The Byzantine NCO model shows rich cyclic behavior, which we demonstrated by showing several examples of graphs with extremely long cycle lengths. For general graphs, we find that the introduction of Byzantine nodes generally increases the probability of cyclic behavior. For networks with a large number of Byzantine nodes, cyclic behavior occurs with a high probability when one opinion holds the absolute majority. Additionally, we found that the introduction of Byzantine nodes also reduces the critical threshold of the NCO model and makes the coexistence of different opinions easier. Both for ER and SF networks, the impact of Byzantine nodes on the final opinion fraction of the NCO model is the largest when Byzantine nodes are selected based on largest degree. Due to the large hubs in SF networks, choosing the hubs as Byzantine nodes has a large impact on the opinion fraction in the steady state.

REFERENCES

- [1] G. Aletti, A. K. Naimzada, and G. Naldi, "Mathematics and physics applications in sociodynamics simulation: the case of opinion formation and diffusion," in *Mathematical Modeling of Collective Behavior in Socio-Economic and Life Sciences*. Springer, 2010, pp. 203–221.
- [2] A. Sîrbu, V. Loreto, V. D. P. Servedio, and F. Tria, "Opinion Dynamics: Models, Extensions and External Effects," *Participatory Sensing, Opinions and Collective Awareness*, p. 363–401, May 2016.
- [3] X. Sun, J. Kaur, S. Milojević, A. Flammini, and F. Menczer, "Social dynamics of science," *Scientific reports*, vol. 3, no. 1, pp. 1–6, 2013.
- [4] K. Sznajd-Weron and J. Sznajd, "Opinion evolution in closed community," *International Journal of Modern Physics C*, vol. 11, no. 06, pp. 1157–1165, 2000.
- [5] T. M. Liggett *et al.*, *Stochastic Interacting Systems: Contact, Voter and Exclusion Processes*. Springer Science & Business Media, 1999, vol. 324.
- [6] S. Galam, "Minority opinion spreading in random geometry," *The European Physical Journal B-Condensed Matter and Complex Systems*, vol. 25, no. 4, pp. 403–406, 2002.
- [7] P. L. Krapivsky and S. Redner, "Dynamics of Majority Rule in Two-State Interacting Spin Systems," *Physical Review Letters*, vol. 90, no. 23, p. 238701, 2003.
- [8] Q. Li, L. A. Braunstein, H. Wang, J. Shao, H. E. Stanley, and S. Havlin, "Non-consensus Opinion Models on Complex Networks," *Journal of Statistical Physics*, vol. 151, no. 1, pp. 92–112, 2013.
- [9] J. Shao, S. Havlin, and H. E. Stanley, "Dynamic Opinion Model and Invasion Percolation," *Physical Review Letters*, vol. 103, no. 1, p. 018701, 2009.
- [10] D. Stauffer and A. Aharony, *Introduction to Percolation Theory*, 2nd ed. Taylor & Francis, 2018.
- [11] Q. Li, L. A. Braunstein, S. Havlin, and H. E. Stanley, "Strategy of competition between two groups based on an inflexible contrarian opinion model," *Physical Review E*, vol. 84, no. 6, p. 066101, 2011.
- [12] F. Rosas, K.-C. Chen, and D. Gündüz, "Social learning for resilient data fusion against data falsification attacks," *Computational Social Networks*, vol. 5, no. 10, 2018.
- [13] H. J. LeBlanc, H. Zhang, S. Sundaram, and X. Koutsoukos, "Consensus of Multi-Agent Networks in the Presence of Adversaries Using Only Local Information," in *Proceedings of the 1st International Conference on High Confidence Networked Systems*, ser. HiCoNS '12. New York, NY, USA: Association for Computing Machinery, 2012, p. 1–10.
- [14] Y. Shang, "Consensus and Clustering of Expressed and Private Opinions in Dynamical Networks Against Attacks," *IEEE Systems Journal*, vol. 14, no. 2, pp. 2078–2084, 2020.
- [15] C. Alcaraz, "Cloud-Assisted Dynamic Resilience for Cyber-Physical Control Systems," *IEEE Wireless Communications*, vol. 25, no. 1, pp. 76–82, 2018.
- [16] B. D. McKay and A. Piperno, "Practical graph isomorphism, ii," *Journal of Symbolic Computation*, vol. 60, pp. 94–112, 2014.